

Characterization of bonding activation sequences to enable ultra-low Cu/SiCN wafer level hybrid bonding

Serena Iacovo
APPM
imec
Leuven, Belgium
Serena.Iacovo@imec.be

Lan Peng
FAB
imec
Leuven, Belgium
Lan.Peng@imec.be

Fuya Nagano
APPM
imec
Leuven, Belgium
Fuya.Nagano@imec.be

Thomas Uhrmann
EVG
EV Group
St. Florian, Austria
T.uhrmann@evgroup.com

Jürgen Burggraf
EVG
EV Group
St. Florian, Austria
J.burggraf@evgroup.com

Andreas Fehkührer,
EVG
EV Group
St. Florian, Austria
A.Fehkührer@evgroup.com

Thierry Conard
MCA
imec
Leuven, Belgium
Thierry.Conard@imec.be

Fumihiko Inoue
APPM
imec
Leuven, Belgium
Fumihiko.Inoue@imec.be

Soon-Wook Kim
3DSIP
imec
Leuven, Belgium
soonugy@naver.com

Joeri De Vos
3DSIP
imec
Leuven, Belgium
Joeri.DeVos@imec.be

Alain Phommahaxay
APPM
imec
Leuven, Belgium
Alain.Phommahaxay@imec.be

Eric Beyne
3DSIP
imec
Leuven, Belgium
Eric.Beyne@imec.be

Abstract—A key factor enabling the reduction of the thermal budget in W2W bonding integration flows is the activation sequence, consisting of cleaning and plasma treatment, used before bonding. For hybrid bonding such activation sequence needs to be selected to fulfill multiple functions: activation of the dielectric bonding surface to obtain a high bonding energy during room temperature bonding, minimize the dielectric bonding annealing temperature while avoiding exposed Cu oxidation and reducing the required annealing temperature for proper Cu-to-Cu bonding. In this paper we discuss the effect of different wafer clean methods (Deionized (DI) water and citric acid) and the effect of different plasma treatments on SiCN and Cu surfaces before bonding. The characterization techniques used include XPS, TEM, ellipsometry, SAM, OES and wafer-to-wafer bond strength testing. It is observed that Nitrogen plasma treatment can help in reducing the CuOx and a mild passivation effect of the surface is observed. Whereas on the Cu pads citric acid, used just before bonding, appears a good option, since clear effectiveness in reducing the CuOx is observed, on the dielectric it may leave some residues which can result sometimes in bonding defects. Moreover, a metric to evaluate efficient SiCN-SiCN bonding is proposed and further understanding of the physical mechanisms involved in SiCN-SiCN bonding are suggested.

Keywords—Wafer-to-wafer bonding, surface activation

I. INTRODUCTION

With the slowdown of Moore's law device scaling, novel approaches are required to increase circuit density, improve circuit performance improvements and decrease power dissipation. 3D integration is enabling new integration schemes, the co-integration of heterogenous functional devices through a variety of direct vertical connections.

The so-called "hybrid bonding" process, where mixed dielectric and metal patterned surfaces are aligned and bonded at room temperature, is an efficient and versatile method to achieve high interconnect density, beyond 1 μm pitch [1] [2] [3].

In previous works imec demonstrated extremely precise fusion wafer to wafer bonding with overlay below 200 nm based on SiCN inorganic dielectric with embedded Cu as a metal. Excellent electrical results have been presented by subjecting the wafer pairs to a total thermal budget of 350 $^{\circ}\text{C}$ [3][1]. At room temperature, the wafer surfaces are bonding through van der Waals forces. The wafer bonding is further strengthened during a low temperature annealing step (250 $^{\circ}\text{C}$) [3]. A reliable Cu-Cu bond only forms when higher temperature anneals are applied (350 $^{\circ}\text{C}$) [3]. Interdiffusion of Cu atoms and grain growth at the bonding interface result in reliable Cu-Cu interconnects. A strong SiCN-SiCN bond strength is important as it will have to withstand the forces during the higher temperature anneal where Cu thermal expansion and grain growth result in large interface stress.

For some applications there is a desire to further reduce such thermal budget because of temperature restrictions on certain materials used in integration flows or to avoid device impact, as for dynamic random access memory (DRAM) [4].

One option to enable a reduction of the Cu-Cu annealing temperature is to modify the Cu pad material properties, such as grain orientation, surface roughness, crystallinity, or material purity. The main hindering factor for good Cu-Cu bonding is the presence of a Copper Oxide (CuO_x) on top of the Cu pads. It is well known that Cu is easily reacting with ambient oxygen resulting in a CuO_x surface layer. This layer is acting as a barrier for pad-to-pad interdiffusion and results in an increased contact resistance. The pre-bonding wafer surface activation sequence, consisting of wafer clean and plasma treatment, can be tuned to minimize the Cu pad oxidation. However, the primary goal of this activation sequence, enhancing the dielectric-to-dielectric bonding, must not be neglected. It is therefore important to monitor the effect not only on Cu but also on the dielectric surfaces.

Different activation sequences, including the use of citric acid clean and various plasma treatments, are analyzed for a variety of surfaces. Bonding of SiCN-SiCN and SiCO-SiCO surfaces is combined with the study of Cu, SiCN and Si surfaces.

Different characterization techniques were used to study of the bonding interfaces: scanning acoustic microscopy (SAM), Mazsara bond strength test, transmission electron microscopy (TEM) coupled with electron dispersive x-ray spectroscopy (EDS) and electron energy loss spectroscopy (EELS). The surfaces have been studied using ellipsometry, atomic force microscopy (AFM), X-ray photoelectron spectroscopy (XPS) and TEM.

By combining the findings gained from these studies, new processes approaches will be developed to allow for a reduction in thermal budget for successful Cu-Cu hybrid bonding.

II. EXPERIMENTAL

A. Test Materials

For the sake of simplicity, the impact of plasma on hybrid surfaces has been characterized separately on SiCN and Cu films deposited on 300 mm wafers. Cu films as well as SiCN films have been prepared according to the actual processes used for hybrid bond. The Cu film has been plated up to 1.6 μm thickness, followed by a 600 nm Cu removal by chemical mechanical polishing (CMP). The SiCN film used for the experiments corresponds to the imec process of reference (POR) material for 3D applications.[5] The SiCN and SiCO films were deposited with a thickness of about 120 nm, they were annealed (densified) and finally polished down to about 100 nm thickness using CMP.

Si wafers with native oxide have been used in parallel to get comparative information by monitoring the thickness and roughness of the plasma-induced oxide layer[6].

B. Activation sequences, plasma recipes and bonding

While for Cu films we mainly tried to evaluate the impact of citric acid (CA) as CuO_x removal agent, for SiCN we also evaluated the impact of changing plasma gases and power.

In the experiments the best-known method (BKM) activation process, which consists of a N_2 plasma activation step followed by a DI-water rinse step, has been compared with other activation processes where either the cleaning recipe was replaced by using a CA-based cleaning recipe after plasma clean (CA post) or by adding an additional CA-based cleaning recipe before the plasma step (CA pre). In the CA-based cleaning recipe, the citric acid was diluted in water and dispensed on the wafer followed by a standard cleaning recipe. Both plasma and wet cleaning processes were performed within the bonding system (EVG GEMINI FBXT). To evaluate the effect of plasma on SiCN, a wide range of plasma gases has been selected. The gases selected were: Nitrogen (N_2), Argon (Ar), Oxygen (O_2), Forming gas (FG), and a mixture of these gases. Power, pressure, flow, and time settings were the same for all the conditions except for two recipes where the power was set at a higher value (indicated by an * in the graph descriptions).

SiCN wafer pairs were bonded at room temperature after using these different pre-bonding recipes and annealed in N_2 at 250 °C. As a reference, a SiCO wafer pair was bonded by using the BKM bonding recipe and annealed at 250 °C.

C. Characterization work and bonding

The effect of the activation sequences on the Cu surfaces have been evaluated using time-controlled experiments in order to minimize the exposure in air of the Cu surface after the treatments. AFM, XPS and TEM measurements were performed within three hours after the surface activation.

AFM (VEECO, Dimension 3100), with a scanning area of 4 mm^2 and measured on two locations, has been used to determine the surface roughness of Cu and Si surfaces after the treatment.

The chemical state of the Cu surfaces has been evaluated on the surface by XPS. The measurements were carried out in Angle Integrated mode using a QUANTES instrument from Physical electronics. The measurements were performed using a monochromatized photon beam of 1486.6 eV. A 100 microns spot was used. The quantification was performed using the Multipak software, using standard sensitivity factors.

To investigate the thickness and the composition of the CuO_x TEM, STEM and EDS analysis have been used. The samples were capped with SoC (Spin-on-Carbon) and ion beam Platinum. Directly after activating the surfaces, samples were cleaved and the capping layer was deposited. During the deposition, the samples were heated to 150 °C for 20-30 seconds. STEM study was done with high-angle annular dark-field (HAADF) and dark-field (DF) detectors by using a Titan tool (FEI).

Part of this characterization work was to evaluate the impact of different plasma recipes at the SiCN-SiCN bonding interface. Scanning acoustic microscopy (SAM) by using an automated

PVA Tepla system was performed in all the cases to verify the presence of voids at the interface. The bond strength has been evaluated by means of Maszara razor blade test. Quality of the bonding interface has been inspected by TEM combined with EDS for a specific case.

Thickness of the SiO₂ on Si wafers induced by the plasma treatment has been characterized before and after the plasma treatment by using the process-line ellipsometer KLA Tencor F5. To verify the presence of particles on blanket wafers after cleaning step KLA Tencor's Surfscan SP3 has been used.

Furthermore, the reactive species generated in the plasma discharge have been observed by using an Optical Emission Spectroscopy (OES) system. The OES is typically acquiring different spectra in different time slots within a discharge process. With the aim of enhancing the possibility to capture differences between different conditions, spectra, belonging to the same discharge, have been added to each other after normalizing each spectrum, at each timestep, to its respective maximum peak (391nm in the case of N₂).

III. RESULTS AND DISCUSSIONS

A. Impact of citric acid pretreatment on Cu and SiCN Surfaces

The Cu surface has been inspected by AFM and XPS in 5 conditions: in the as-prepared state, after cleaning with a citric acid solution (CA clean), after activating with the BKM sequence and after a CA post activation sequence. Fig.1 shows a comparison of AFM measurements where the root mean squared roughness (Rq) is represented for each condition. The error bar indicated is main related to the wafer-level variations. It can be noticed that in the as-prepared status, the Cu surface shows the highest roughness characterized by the largest variation across the wafer surface. That could point out to a non-uniform growth of the CuOx on the wafer surface[6]. Variation is strongly reduced for the sample subjected to a BKM activation sequence is used.

The surface gets significantly smoother for the sample cleaned with CA and also the variation is reduced. A lower roughness is proven to be an important property to minimize thermal budget [7]

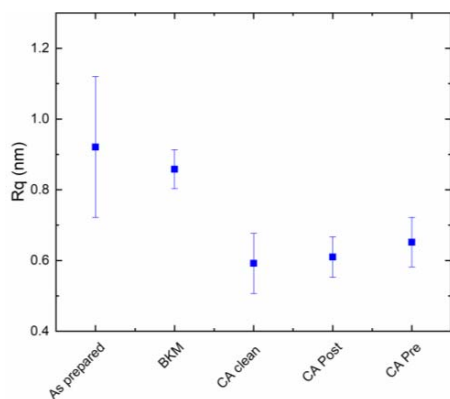


Fig. 1: Measured RMS roughness of Cu surfaces measured by AFM before and after various treatments.

B. Chemical state of the Cu surface

The chemical composition of Cu surface has been assessed by XPS. Figures 2 to 5 show the Cu 2p_{3/2}, C 1s, N 1s and Cu LM2 spectra, respectively, from the different samples. For the as-prepared Cu sample the spectrum in Fig. 2 exhibits two peaks at 932.5 and 934.6 eV, which are attributed to metallic Cu and Cu²⁺. Also, a pronounced satellite structure between 938 and 945 eV is observed, associated to Cu²⁺. The Cu²⁺ features are indicative of the presence of CuO and Cu carbonate/hydroxide, resulting from a Cu oxidation in air[8].

A strong reduction of these features can be observed in the remaining samples. The reduction is strongest whenever citric acid is used.

In Fig. 3 the C1s spectrum is presented. A peak at ~289 eV, which could be assigned to CO₂, is shifting towards more negative values in the CA post and in the CA clean samples. This could indicate the presence of COH on the surface which might indicate the presence of citric acid residues on the surface[7]. However, we do not observe the same behaviour for the sample where CA is used at the beginning of the sequence (CA pre).

In Fig. 4, the Nitrogen region is presented for 3 samples, it is possible to observe a line at ~397.5 eV which could be assigned to Cu-N[8] proving that Nitrogen is reacting with the Cu during the activation. Yet, concentration of Nitrogen calculated by XPS is around ~4% probably not enough to passivate efficiently the entire Cu surface. As a matter of fact, if we have a look at the Cu LMM peak Fig. 5 we see that the ratio between metallic Cu and CuOx is low for the BKM and CA pre samples. And the most efficient recipe is the one where citric acid is applied at the end of the activation sequence. Nevertheless, we believe that XPS results, on their own, are not enough to make a definite conclusion about the reduction of Cu oxide after plasma treatment considering also the uncertainty related to the presumably Cu oxidation during the sample preparation and transportation from the cleaning chamber to the XPS spectrometer.

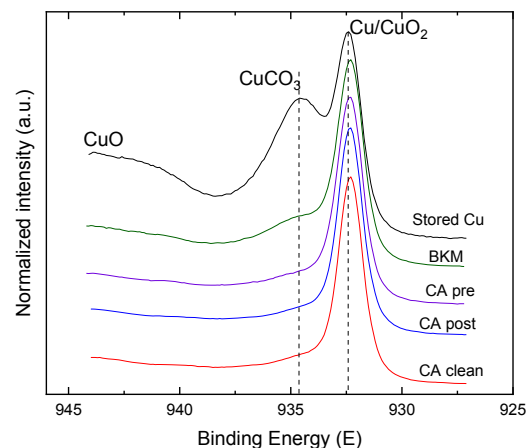


Fig. 2: Overlay Cu2p3, presented in angle integrated mode-graphs are auto-scaled to enable chemical comparison

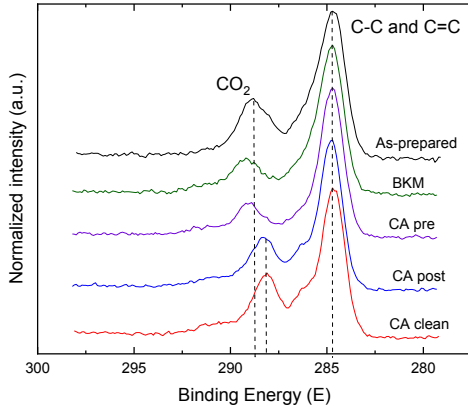


Fig. 3: Overlay C1s, presented in angle integrated mode-graphs are auto-scaled to enable chemical comparison

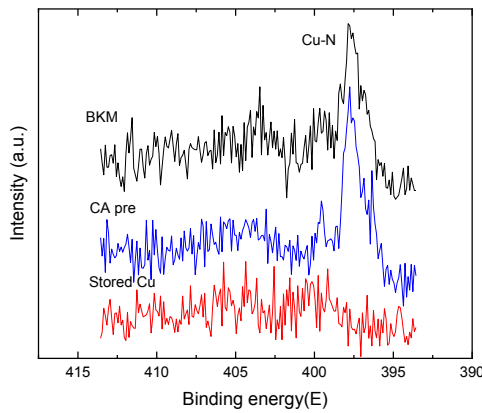


Fig. 4: Comparison of N1s spectra acquired for 3 surface conditions

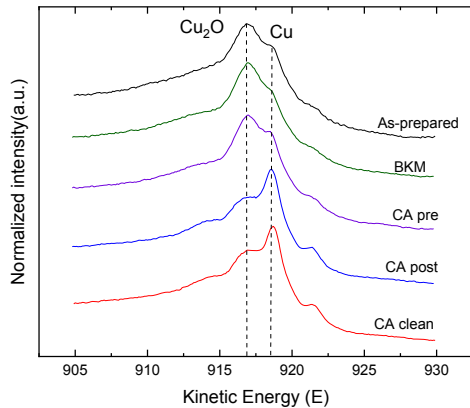


Fig. 5: Overlay Cu2p, presented in angle integrated mode-graphs are auto-scaled to enable chemical comparison

C. Reactivity of the Cu surface

TEM inspection has been used to verify indirectly the reactivity of the surface in 3 conditions (in the as-prepared case, the BKM and after CA post). As mentioned before the samples

have been heated to 150 °C for 20-30 seconds to deposit the capping layer. At this temperature thermal oxidation of Cu is known to start[9]. Therefore, we can expect to observe a worst-case scenario of surface oxidation considering that the bonding it happens at room temperature immediately after the activation process.

For the as-prepared sample the TEM analysis confirmed the presence of a rough morphology. The as-prepared surface appeared rougher compared to the remaining samples.

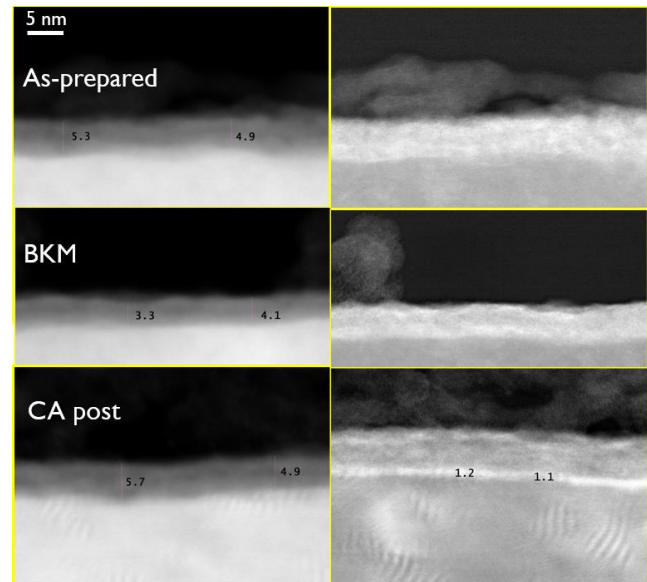


Fig. 6: HAADF STEM pictures (left column) and DF-STEM images (right column) measured for the Cu samples in the as-prepared state (1st row) after a BKM activation sequence(2nd row) and after a CA-post activation sequence(3rd row).

The oxide layer visible in the STEM HAADF images in Fig.6, it is ranging from 4.6 nm to 5.3 nm in the as-prepared sample, from 3.3nm to 4.1 nm in the BKM sample and from 4.9 to 5.5 nm in the CA post sample. The fact that in a worst-case scenario situation the CuOx layer appears thinner when the layer is subjected to the BKM recipe it is confirming a partial nitrogen passivation of the Cu surface observed in the XPS analysis.

The results of the sample subjected to CA post sequence is pointing to a fast oxidation mechanism occurring after the treatment. Key when using such a process would be the minimization of waiting time between activation and bonding.

In DF-STEM image for sample CA post a bright layer can be distinguished at the CuOx/Cu interface. EDS analysis shows a small Carbon peak in this area which might be attributed to citric acid residues, confirming the XPS interpretation.

Results are confirming a cleaning action performed by the plasma treatment on Cu surfaces.

D. Effect of citric acid on SiCN

The bond strength achieved at the SiCN-SiCN interface when using the BKM the CA pre and CA post activation sequences are shown in the inset of Fig.7 together with SAM pictures with a resolution of 30 $\mu\text{m}/\text{pixels}$. It can be observed that by using CA-based activation sequences the bond strength is slightly lower.

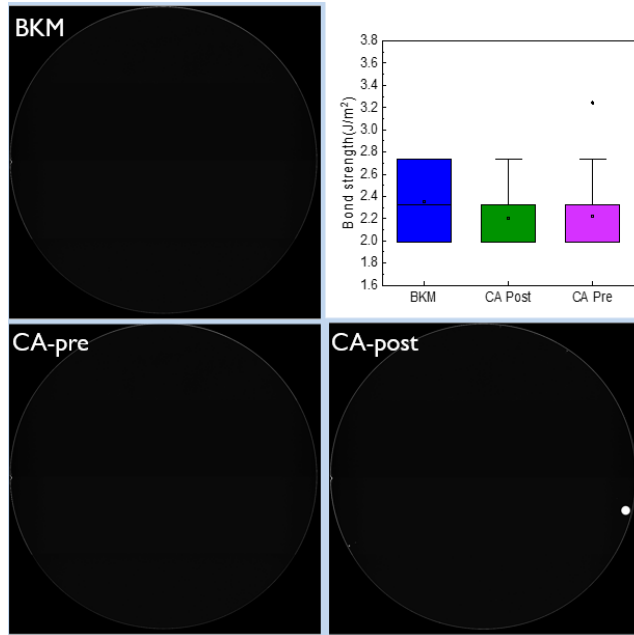


Fig. 7: SAM inspection after W2W bonding of SiCN-SiCN interfaces when using the BKM the CA pre and CA post activation sequences. Top right: Measured bond energy

The particle contamination on blanket Si wafers has been monitored on a regular basis during a one-year period, allowing for a comparison of the standard clean and after CA-based cleaning. It is observed that after citric acid clean process we deposit on average 24 particles larger than 160 nm while by using only standard clean this is limited to an average of 5 particles on a 300mm wafer. In the case of CA-based cleaning the diameter of the particles is most of the times below 1 μm . Voids induced by such small particles are likely not observed in SAM scans due to its limited resolution.

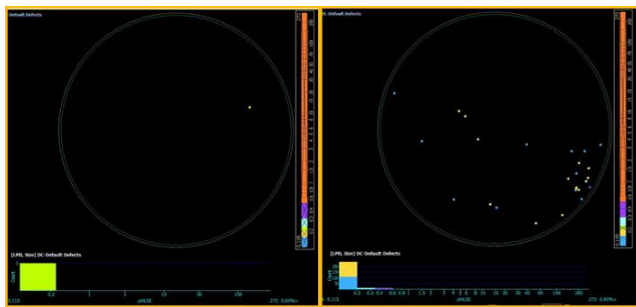


Fig. 8: Typical SP3 maps observed after a standard clean (left side) and after a CA-based clean (right side).

E. Interface

The interface of SiCO-SiCO bonded pair has been inspected using TEM and EDS analysis. As can be seen from Fig.9, three interfacial layers exhibiting different contrasts in the HAADF-STEM images (dark/bright/dark) are observed at the bonding interface. From the EDS analysis a low amount of N is detected in the SiOx/SiCO interfacial layers identifying the layers stack as: SiCO/SiCNO/SiOx/SiCNO/SiCO. It is inferred that N is embedded on the surface of the SiCO film during the activation. Note that a similar analysis of SiCN-SiCN bonded surfaces would not allow us to make this observation as N is already present in those films, hence the use of SiCO-SiCO bonding for this part of the study.

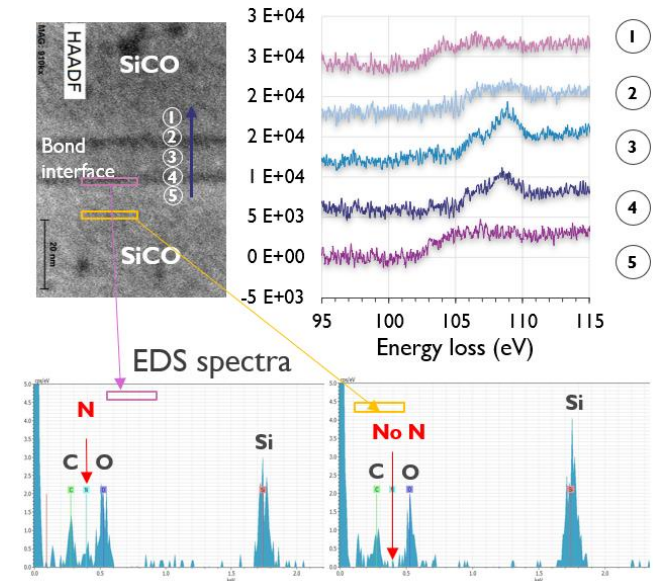


Fig. 9: Detailed analysis by HAADF-TEM, EELS and EDS of the SiCO-SiCO wafer bonding interface.

F. Plasma effect at the interface of SiCN and on Si surfaces

Bond strength results as a function of the different plasma recipes tested are shown in Fig. 10. The highest results have been achieved when using the BKM recipe and when using the Ar-O₂ plasma recipe while the lowest when using Ar/FG and a more complex recipe where Ar/O₂ followed FG/Ar is used. The latter recipes were characterized by a higher plasma power compared to the remaining recipes. The measurement error inherent with this technique does not allow us to draw strong conclusions regarding optimum recipes. The most significant parameter which was shown to affect to bonding energy is the plasma power. The type of gas used appears to have only a secondary effect, given the measurement uncertainties.

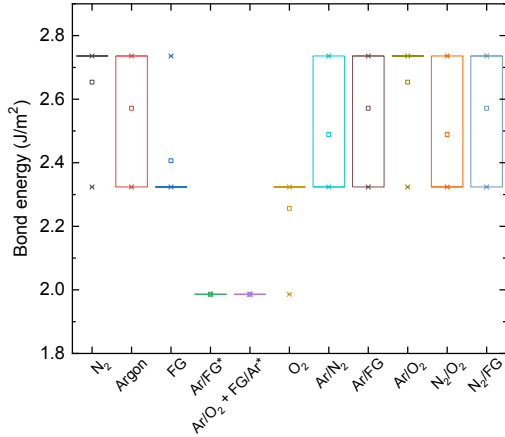


Fig. 10: Measured wafer-to-wafer bonding energy of the different pre-treatment experiments.

As explained in the previous section Si wafers have been subjected to the same plasma treatments to monitor the roughness and thickness of the plasma induced SiO₂ layer. The thickness of the native oxide was calculated to be ~1.4 nm for all the wafers while initial data RMS roughness before plasma were in the range of 0.11 to 0.13 nm. The surface roughness below and after plasma processing is shown in Fig. 11.

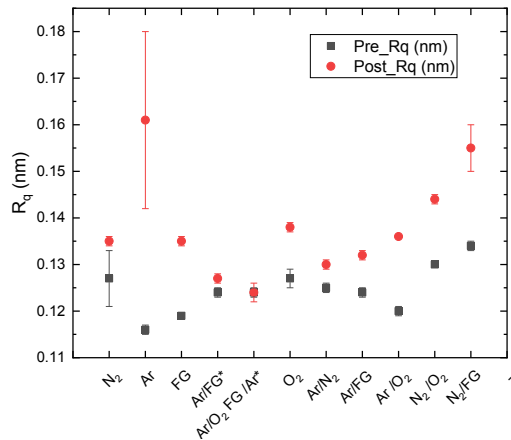


Fig. 11: Si surface roughness before and after plasma processing

In Fig. 12, the measured oxide thickness is correlated to the surface roughness. The process induced oxide is generally in the 4 to 4.5 nm range, except for two cases where a thickness of ~6.5 nm is measured. It can be observed that the wafer pairs which shows a clear weaker interface strength can be associated to a recipe which induced the thickest oxide growth and characterized by the highest plasma power.

The thickest oxides were also the ones exhibiting the smoothest surface and the Rq measured after plasma was comparable to the roughness measured on the same wafer before subjecting it to plasma activation. Since these two recipes were the ones which were characterized by the highest power, we can imagine that the plasma damage was such that a strong oxidation occurred leading to the creation of an energetically inert self-reconstructed layer similar to the native oxide. If we would

support the sputtering effect of the plasma, we could conclude that too many defects are created leading to an excessive absorption of water. Such method could represent a metric to evaluate the efficiency of the plasma treatment for SiCN bonding.

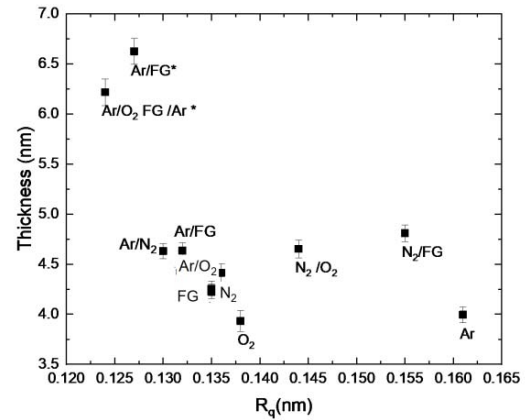


Fig. 12: Correlation of oxide thickness and surface roughness for different plasma pre-treatment conditions

The creation of an oxidized layer, not corresponding to a pure oxide layer[5], after plasma treatment has been observed also for SiCN substrates [10]. After plasma activation the TEM analysis shows a layer which is ~ 1.4 nm before plasma and ~6.3 nm after plasma activation. As for the TEM inspection of the CuOx, we should not neglect in this case the impact of the sample preparation on the measured oxide thickness. It follows that what we observe in the TEM image is thicker compared to what we would observe at room temperature.

Using ellipsometry a model has been created to calculate the composite layer thickness on top of the SiCN. The thickness of this layer is estimated to be ~ 2.8 nm after BKM plasma activation (Fig.13), therefore thinner to what we achieve on the Si substrate. Probably meaning that water penetration in the case of SiCN would be limited to a shallower portion of the surface.

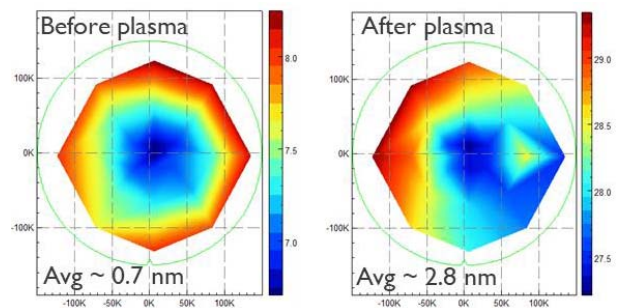


Fig. 13: Ellipsometry measurement of the SiCN surface layer thickness, before and after plasma processing. To be noticed that after plasma treatment the non-uniformity of the oxidized layer is within 0.15 nm.

It has been demonstrated in the past that the superiority of SiCN as bonding dielectric compared to SiO₂ lies in the different physical bonding mechanisms. While for SiCN a significant role in strengthening the bond strength is played by a high amount of

DBs generated during plasma, for SiO₂ no DBs are observed after plasma activation. In this respect a high amount of water on the surface would counteract the DBs driven mechanism activated upon annealing.

G. Plasma effect on SiCN and Si

In Fig. 14 a representative OES spectrum obtained when using a BKM plasma recipe is shown. Different nitrogen-plasma emission peaks are observed. The strongest emission peak in the spectrum occurs at emission wavelengths of 391 nm which, together with the sharp peak at 428 nm, is related to the molecular N²⁺ ion. Also, different sharp nitrogen-plasma emission peaks associated with neutral nitrogen molecules are visible [13].

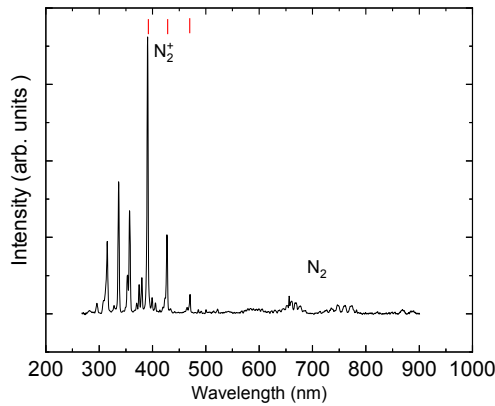


Fig. 14: OES spectrum BKM plasma recipe.

The absence or relative low concentration of atomic N suggest that the possible passivation behavior observed in the XPS spectra could be due to N ions implanted or absorbed on the surface.

No significant differences could be observed in the spectra acquired when three different substrates were loaded in the chamber and when using the same plasma recipe. In Fig.15 the different spectra generated when different substrates were present are compared. The Cu, Si, SiCN1 and SiCN2 spectra have been recorded during a N₂ activation step when a Cu, Si and 2 different SiCN substrates were present in the chamber, respectively.

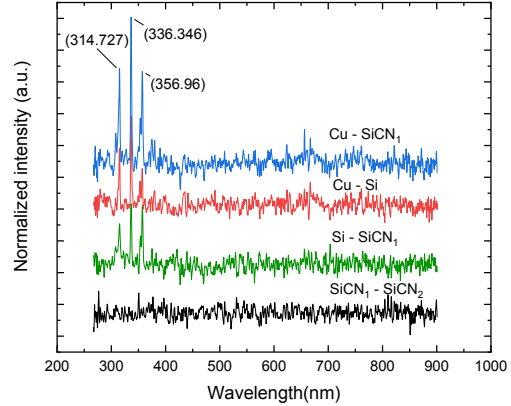


Fig. 15: OES spectra during plasma pre-processing for different wafer surfaces.

It can be observed that if the same kind of substrate is present in the chamber no enhanced peaks can be observed but only a noisy background. However, when we look at the differences obtained when different substrates are present in the chamber, we can recognize more enhanced peaks at 315, 337 and 357 nm wavelengths. Such peaks can be assigned to CH, NH, and CN. These are typical by-products from reaction in a chemical sputtering process. However, a unique assignment cannot be done since emission bands of NH, CH and CN are overlapping with the N₂ emission band.

Even if by OES we could not clearly observe by-products originating from possible physical or chemical reactions the characterization study performed on the different materials is pointing to a particularly reactive process where a cleaning action is observed on Cu to remove Copper hydroxide Cu(OH)₂ and copper carbonate CuCO₃ which are known to be present on Cu₂O and CuO due to the adsorption of water and carbon dioxide from air [11].

Additionally, creation of defects due to plasma processing are responsible for the increased hydrophilicity which, in turn enhances the growth of an oxidized layer several hours after the plasma treatment. The thickness of this reconstructed layer is seen to give information regarding the damage created during plasma.

A thinner reconstructed layer is measured for SiCN compared to SiO₂ enforcing the view of a different physical bonding mechanism behavior previously observed for SiCN[12].

IV. CONCLUSIONS

A cleaning action of the plasma processes on Cu surfaces has been observed. At the same time defects are created which can react with plasma species, as it has been observed for N on Cu surfaces and at the interface of SiCO/SiCO. Similarly, defects can react with the environment if the surface is kept long enough in air after the plasma process, generating an oxidized layer which can be measured on top of Si surfaces but also on SiCN surfaces. On SiCN surfaces a thinner oxidized layer compared to the one observed for Si is measured by ellipsometry.

A possible way to monitor the surface modification after plasma would consist in monitoring the oxide growth on Si wafers induced by plasma activation. Thicker oxide layers, caused by higher power plasma recipes, appear to be correlated with a weaker SiCN-SiCN interface.

It follows that for a successful SiCN-SiCN bonding defects creation must be limited to efficiently allow the first part of the bonding process, happening at room temperature and driven by the hydrophilicity of the surface, without counteracting with the following steps activated upon annealing where the dangling bonds are playing an important role in strengthening the bond strength.

A promising activation sequence which would allow a further reduction of CuOx compared to the BKM recipe is identified. This consists in the use of citric acid as cleaning process before plasma activation followed by a wet cleaning process. For this activation sequence Cu roughness is clearly reduced, void free SiCN-SiCN bonding is obtained. However, the cleaning recipe must be further optimized to reduce the number of particles left on the surface.

ACKNOWLEDGMENT

The author would like to thank Paola Favia and Maxim Korytov for the detailed TEM analysis. This work is carried within the frame of the imec 3D System Integration Industrial Affiliation Program and within a Joint Development Project between imec and EVG.

REFERENCES

- [1] E. Beyne *et al.*, "Scalable, sub 2 μ m pitch, Cu/SiCN to Cu/SiCN hybrid wafer-to-wafer bonding technology," *Tech. Dig. - Int. Electron Devices Meet. IEDM*, pp. 32.4.1-32.4.4, 2018, doi: 10.1109/IEDM.2017.8268486.
- [2] L. Arnaud *et al.*, "Fine pitch 3D interconnections with hybrid bonding technology: From process robustness to reliability," *IEEE Int. Reliab. Phys. Symp. Proc.*, vol. 2018-March, pp. 4D.41-4D.47, 2018, doi: 10.1109/IRPS.2018.8353591.
- [3] S. W. Kim *et al.*, "Novel Cu/SiCN surface topography control for 1 μ m pitch hybrid wafer-to-wafer bonding," *Proc. - Electron. Components Technol. Conf.*, vol. 2020-June, pp. 216-222, 2020, doi: 10.1109/ECTC32862.2020.00046.
- [4] M. Chang *et al.*, "Si - H bond breaking induced retention degradation during packaging process of 256 Mbit DRAMs with negative wordline bias," *IEEE Trans. Electron Devices*, vol. 52, no. 4, pp. 484-491, 2005, doi: 10.1109/TED.2005.844743.
- [5] F. Inoue *et al.*, "Influence of Composition of SiCN as Interfacial Layer on Plasma Activated Direct Bonding Influence of Composition of SiCN as Interfacial Layer on Plasma Activated Direct Bonding," 2019, doi: 10.1149/2.0241906jss.
- [6] T. Plach, K. Hingerl, S. Tollabimazraehno, G. Hesser, V. Dragoi, and M. Wimplinger, "Mechanisms for room temperature direct wafer bonding," *J. Appl. Phys.*, vol. 113, no. 9, 2013, doi: 10.1063/1.4794319.
- [7] M. Favaro, H. Xiao, T. Cheng, W. A. Goddard, and E. J. Crumlin, "Subsurface oxide plays a critical role in CO₂ activation by Cu(111) surfaces to form chemisorbed CO₂, the first step in reduction of CO₂," *Proc. Natl. Acad. Sci. U. S. A.*, vol. 114, no. 26, pp. 6706-6711, 2017, doi: 10.1073/pnas.1701405114.
- [8] H. Seo, H. Park, and S. E. Kim, "Comprehensive Analysis of a Cu Nitride Passivated Surface That Enhances Cu-to-Cu Bonding," *IEEE Trans. Components, Packag. Manuf. Technol.*, vol. 10, no. 11, pp. 1814-1820, 2020, doi: 10.1109/TCPMT.2020.3024998.
- [9] S. Choudhary *et al.*, "Oxidation mechanism of thin Cu films: A gateway towards the formation of single oxide phase," *AIP Adv.*, vol. 8, no. 5, 2018, doi: 10.1063/1.5028407.
- [10] L. Peng *et al.*, "Pre-bonding Characterization of SiCN Enabled Wafer Stacking," vol. 155, no. 12, p. 3001, 2019.
- [11] M. R. Baklanov *et al.*, "Characterization of Cu surface cleaning by hydrogen plasma," *J. Vac. Sci. Technol. B Microelectron. Nanom. Struct.*, vol. 19, no. 4, p. 1201, 2001, doi: 10.1116/1.1387084.
- [12] L. Peng *et al.*, "Advances in SiCN-SiCN Bonding with High Accuracy Wafer-to-Wafer (W2W) Stacking Technology," pp. 2018-2020, 2018.